Available online at www.sciencedirect.com
ScienceDirect
Metabolism Clinical and Experimental 59 (2010) 1057–1064
Metabolism
Clinical and Experimental
www.metabolismjournal.com

The characterization of Abelson helper integration site–1 in skeletal muscle and its links to the metabolic syndrome

Matthew J. Prior[a,1,2], Victoria C. Foletta[a,2], Jeremy B. Jowett[b], David H. Segal[a], Melanie A. Carless[c], Joanne E. Curran[c], Tom D. Dyer[c], Eric K. Moses[c], Andrew J. McAinch[d], Nicky Konstantopoulos[a], Kiymet Bozaoglu[a], Greg R. Collier[e], David Cameron-Smith[a], John Blangero[c], Ken R. Walder[a,f,*]

[a]*School of Exercise and Nutrition Sciences, Deakin University, Geelong 3217, Australia*
[b]*The Baker IDI Heart and Diabetes Institute, Melbourne 8008, Australia*
[c]*Southwest Foundation for Biomedical Research, San Antonio, TX 78227, USA*
[d]*School of Biomedical and Health Sciences, Victoria University, Melbourne 8001, Australia*
[e]*ChemGenex Pharmaceuticals Ltd, Geelong 3220, Australia*
[f]*Verva Pharmaceuticals Ltd, Geelong 3220, Australia*

Received 10 June 2009; accepted 2 November 2009

Abstract

The human Abelson helper integration site–1 (AHI1) gene is associated with both neurologic and hematologic disorders; however, it is also located in a chromosomal region linked to metabolic syndrome phenotypes and was identified as a type 2 diabetes mellitus susceptibility gene from a genomewide association study. To further define a possible role in type 2 diabetes mellitus development, AHI1 messenger RNA expression levels were investigated in a range of tissues and found to be highly expressed in skeletal muscle as well as displaying elevated levels in brain regions and gonad tissues. Further analysis in a rodent polygenic animal model of obesity and type 2 diabetes mellitus identified increased Ahi-1 messenger RNA levels in red gastrocnemius muscle from fasted impaired glucose–tolerant and diabetic rodents compared with healthy animals ($P < .002$). Moreover, elevated gene expression levels were confirmed in skeletal muscle from fasted obese and type 2 diabetes mellitus human subjects ($P < .02$). RNAi-mediated suppression of Ahi-1 resulted in increased glucose transport in rat L6 myotubes in both the basal and insulin-stimulated states ($P < .01$). Finally, single nucleotide polymorphism association studies identified 2 novel AHI1 genetic variants linked with fasting blood glucose levels in Mexican American subjects ($P < .037$). These findings indicate a novel role for AHI1 in skeletal muscle and identify additional genetic links with metabolic syndrome phenotypes suggesting an involvement of AHI1 in the maintenance of glucose homeostasis and type 2 diabetes mellitus progression.

1. Introduction

The murine Ahi-1 gene locus is a proviral integration site associated with the development of viral-induced murine leukemias and lymphomas [1,2]. In humans, Abelson helper integration site–1 (AHI1) is linked to leukemia development [2] as well as to several neurologic disorders including schizophrenia [3,4] and Joubert syndrome, an autosomal recessive brain malformation [5,6]. AHI1 is a large protein containing multiple protein-protein interaction domains including Src homology 3 and WD40-repeat domains, and proline-rich regions [7], which are often present in proteins involved in signal transduction and cytoskeletal organization [8-10], and was recently described to interact with BCR-ABL and JAK2 and modulate their phosphorylation levels in leukemic cells [11]. These features suggest that AHI1 has the potential to act as both a scaffold and signaling protein.

* Corresponding author. School of Exercise and Nutrition Sciences, Deakin University, Geelong, Australia. Tel.: +61 3 5227 2883; fax: +61 3 5227 2170.
E-mail address: walder@deakin.edu.au (K.R. Walder).
[1] Present address: Diabetes and Obesity Research Program, Garvan Institute, Sydney, Australia.
[2] These authors contributed equally.

0026-0495/$ – see front matter © 2010 Elsevier Inc. All rights reserved.
doi:10.1016/j.metabol.2009.11.002

In addition to its associations with neurologic and hematologic disorders, prior studies have linked 6q23, the AHI1 chromosomal region, to type 2 diabetes mellitus (T2D) [12] and to insulin resistance and metabolic syndrome–related phenotypes [13,14] including fasting blood glucose levels in Mexican Americans [15]. Furthermore, the AHI1-LOC441171 gene locus was identified as a T2D susceptibility gene region after a genomewide association study (GWAS) in European populations [16]. A GWAS is a powerful approach to identify novel genomic regions associated with complex diseases, and at least 6 new gene regions have been linked to the risk of T2D by GWASs in recent times [17]. Two single nucleotide polymorphisms (SNPs) from the AHI1-LOC441171 gene region remained the most significantly associated out of 10 SNPs further investigated in a replication study [16]. However, a follow-up study was not able to replicate the same SNPs from a study in a Danish population [18], making it unclear as to whether a role for the AHI1 gene in the development of T2D and metabolic syndrome exists. Here, we sought to identify novel biological or further genetic evidence for Ahi-1/AHI1 in the metabolic syndrome. We measured Ahi-1/AHI1 messenger RNA (mRNA) expression in both insulin-sensitive and insulin-resistant tissues from an animal model of obesity and T2D, and verified significant gene expression changes in humans. We examined the effects of reduced Ahi-1 levels on glucose transport in L6 myotubes and also investigated a range of AHI1 SNPs in a sample of Mexican American subjects to determine if any were associated with fasting blood glucose levels.

2. Materials and methods

2.1. Human and animal research

All human and animal experimental procedures were approved by the Deakin University ethics committee; and for the human study, informed written consent was obtained from each participant. *Psammomys obesus* animals were housed at Deakin University and maintained at 22°C ± 1°C with a 12-hour–light, 12-hour–dark cycle. When fed ad libitum a standard laboratory diet from which 63% of energy was derived from carbohydrate, 25% from protein, and 12% from fat (Barastoc, Victoria, Australia), a proportion of *P obesus* display a range of metabolic responses including obesity, dyslipidemia, insulin resistance, and T2D [19-21]. At 16 weeks of age, animals were classified as lean and normal glucose tolerant (NGT), obese and impaired glucose tolerant (IGT), or obese and T2D according to circulating plasma insulin levels, blood glucose levels, and body weight as previously described [19,21]. At 18 weeks of age, fed and animals fasted for 24 hours were killed by anesthetic overdose (120 mg/kg of pentobarbitone; Sigma Chemical, St Louis, MO). See Table 1 for the body weight, plasma insulin, and whole blood glucose levels of the animals used for this study. Human participants consisting of 10 lean (3 male, 7 female), 13 obese (1 male, 12 female), and 9 obese T2D (6 male, 3 female) subjects were fasted for 12 to 18 hours before skeletal muscle biopsies were taken from the vastus lateralis. See Table 2 for the subjects' age, weight, body mass index, fasting blood glucose, and fasting plasma insulin phenotypic characteristics. All biopsies and tissues were snap frozen in liquid nitrogen and stored at −80°C. Whole blood glucose levels were measured using an enzymatic glucose analyzer (model 27; Yellow Springs Instruments, Yellow Springs, OH), and plasma insulin concentrations were determined using an insulin double-antibody radioimmunoassay kit (Linco Research, St Charles, MO).

Table 1
Phenotypic characteristics of fed and 24-hour fasted NGT, IGT, and T2D *P obesus*

Characteristic		NGT	IGT	T2D
Weight (g)	Fed (n = 6)	192.6 ± 7.7	227.6 ± 7.1*	238 ± 6.6*,†
	Fasted (n = 7)	194.8 ± 8.2	225.9 ± 8.2*	237 ± 6.6*,†
BG (mmol/L)	Fed (n = 6)	4.3 ± 0.2	4.5 ± 0.3	13.5 ± 1.2*,†
	Fasted (n = 6)	3.4 ± 0.3	3.6 ± 0.3	5.1 ± 0.3*,†
PI (μU/L)	Fed (n = 6)	80.7 ± 10.9	407.4 ± 85.2*	481.3 ± 78.2*
	Fasted (n = 7)	21.3 ± 3.2	119.5 ± 28.1*	173.8 ± 59*

Data presented as mean ± SEM. BG indicates blood glucose; PI, plasma insulin.
* $P < .05$ to NGT values.
† $P < .05$ to IGT values.

Table 2
Phenotypic characteristics of fasted lean, obese, and T2D human subjects

Characteristic	Lean (n = 10)	Obese (n = 13)	T2D (n = 9)
Age (y)	44.1 ± 1.6	36.2 ± 2.2*	51.1 ± 2.3*,†
BMI (kg/m^2)	22.6 ± 0.8	46.4 ± 1.9*	40.0 ± 1.0*,†
Weight (kg)	66.7 ± 4.0	123.7 ± 5.0*	121.8 ± 7.2*
FBG (mmol/L)	5.0 ± 0.3	5.1 ± 0.1	7.7 ± 0.8*,†
FPI (μU/L)	7.9 ± 3.0	16.6 ± 1.2*	27.2 ± 2.8*,†

Data presented as mean ± SEM. BMI indicates body mass index; FBG, fasting blood glucose; FPI, fasting plasma insulin.
* $P < .05$ to lean values.
† $P < .05$ to obese values.

2.2. Cell culture and small interfering RNA transfection

Rat L6 myoblasts were a gift from Prof A Klip (The Hospital for Sick Children, Toronto, Ontario, Canada) and were maintained in 25 mmol/L glucose Dulbecco minimum essential medium (HG DMEM) (Invitrogen, Melbourne, Victoria, Australia) with 10% fetal calf serum (Invitrogen) at 37°C in 5% CO_2. When confluent, myoblasts were differentiated in HG DMEM plus 2% fetal calf serum (differentiation medium) for 3 days before transfection with 25 nmol/L small interfering RNAs (siRNAs; Silencer siRNA Construction Kit; Ambion, Austin, TX) using Lipofectamine

2000 (Invitrogen) in serum-free Opti-MEM (Invitrogen). The Ahi-1–specific siRNA sequence used in this study was 5′-aagaaagaugacagugagcgu and 5′-aaacgcucacugucaucuuuc for the siAhi-1 antisense and sense strands, respectively. To control for siRNA transfection effects, a negative control siRNA (siNeg) was used. The antisense and sense sequences were 5′-aaguaucuagguacacacuca and 5′-aaugaguguguacguagauac, respectively. The cells were harvested for gene expression analysis and for 2-deoxyglucose transport assays 48 hours posttransfection.

2.3. 2-Deoxyglucose transport

2-Deoxy-D-[1-^{3}H] glucose transport measurements were carried out as previously described [22] with minor modifications. After a 4-hour starvation in serum-free HG DMEM, L6 myotubes were incubated at 37°C in Krebs-Ringer phosphate buffer for 30 minutes with 0 or 100 nmol/L insulin (HumulinR; Eli Lilly, Indianapolis, IN). 2-Deoxyglucose (1 mCi/mL; Amersham Biosciences, Buckinghamshire, United Kingdom) at a final concentration of 50 μmol/L was added to the cells; and after 10 minutes, glucose transport was stopped by the addition of ice-cold phosphate-buffered saline. Cells were washed 3 times in phosphate-buffered saline before lysis with 0.01% sodium dodecyl sulfate (SDS) and counting for ^{3}H incorporation. Glucose transported was calculated as picomoles of glucose per minute.

2.4. Real-time polymerase chain reaction

Total RNA was extracted and isolated using TRIzol (Invitrogen) and RNeasy mini kit columns (Qiagen, Chatsworth, CA), respectively. The RNA quality and quantity were assessed using the RNA 6000 Nano Assay kit and the Agilent 2100 Bioanalyzer (Agilent Technologies, Waldbronn, Germany). The first-strand complementary DNA was generated using the Superscript II First-Strand Synthesis System (Invitrogen). Primers for real-time polymerase chain reaction (PCR) analyses were as follows: Rat Ahi-1 (5′-agagcttcgtcaactccatctgt and 5′-cgatgacgccgatgca), *P obesus* Ahi-1 (5′-actgctcaaagtatcgtactgttcattagt and 5′-cagcggtgcaattctgatgta), human AHI1 (5′-atggatctccggatattagtagcaa and 5′-aaaagtcccacatggagtcaaagta), rat cyclophilin (5′-cccaccgtgttcttcgaca and 5′-ccagtgctcagagcacgaaa), *P obesus* cyclophilin (5′-cccaccgtgttcttcgaca and 5′-ccagtgctcagagcacgaaa), and human cyclophilin (5′-catctgcactgccaagactga and 5′-ttcatgccctcctttcactttgc). Real-time PCR was performed on an ABI PRISM 7700 sequence detector (Applied Biosystems, Foster City, CA) using SYBR Green PCR master mix (Applied Biosystems) using the following conditions: 95°C for 10 minutes (1 cycle), 95°C for 30 seconds, and 60°C for 1 minute (40 cycles).

2.5. Immunoblotting analysis

Immunoblotting was performed as essentially described previously [23]. Briefly, cells were lysed in ice-cold radioimmunoprecipitation assay buffer (50 mmol/L Tris HCl, pH 7.4, 150 mmol/L NaCl, 1% NP-40, 0.5% sodium deoxycholate, 0.1% SDS) containing protease inhibitors (2 μg/mL aprotinin, 10 μg/mL leupeptin, 1 μg/mL pepstatin A, and 1 mmol/L phenylmethylsulfonyl fluoride) and phosphatase inhibitors (10 nmol/L sodium fluoride and 1 mmol/L sodium orthovanadate) before centrifuging at 13 000*g* for 20 minutes at 4°C to remove insoluble material. The protein concentration was determined using Bio-Rad protein assay reagent (Bio-Rad Laboratories, Gladesville, NSW, Australia), and 20 μg of total protein was separated by SDS–polyacrylamide gel electrophoresis before transferring to polyvinylidene difluoride membranes and immunoblotting with anti-Akt (1:1000; Cell Signaling Technology, Danvers, MA) or with anti–phospho-Akt Ser473 (1:1000, Cell Signaling) for 1 hour at room temperature. Detection of the primary antibodies was performed using an anti-rabbit immunoglobulin G, horseradish peroxidase–linked antibody (1:5000; GE Healthcare, Rydalmere, New South Wales, Australia) and developed in ECL chemiluminescence reagent (GE Healthcare). The ChemiGeniusII gel documentation system and Gene Snap software (Syngene, Cambridge, United Kingdom) were used to visualize protein bands, and densitometry was performed with Gene Tools software (Syngene).

2.6. Statistical analysis used for in vitro data

Gene expression and phenotypic data are expressed as the mean ± SEM and were analyzed using SPSS 14.0 software (Fullerton, CA). All data were subjected to Kolmogorov-Smirnov test for normality, and statistical differences were assessed using unpaired Student *t* test for 2-group comparisons. For the statistical analysis of more than 2 groups, data were subjected to a 1-way analysis of variance with post hoc least significance difference tests when variances were equal. Statistical significance was defined as $P < .05$.

2.7. Human association study

The Institutional Review Board of the University of Texas Health Science Center at San Antonio approved all protocols, and informed consent was obtained from all subjects. The Illumina Sentrix HumanHap550 Genotyping BeadChip (San Diego, CA) was used to genotype 565 Mexican American subjects from the San Antonio Family Heart Study [24]. Of the 565 individuals, 199 were male and 366 were female from 18 to 81 years. A total of 75 (13.3%) of these individuals had T2D and were excluded from the analyses of fasting glucose. Association analysis was performed using the measured genotype approach [25] allowing for nonindependence among family members. To account for multiple tests, we calculated the effective number of SNPs (tests) using a previously described method [26] based on the pattern of linkage disequilibrium among SNPs. The mean normalized fasting plasma glucose levels to determine the direction of effect of the SNP genotypes were generated by inverse normalization using the computer package SOLAR (http://solar.sfbrgenetics.org/).

2.8. Statistical genetic methods used in human cohort

Before genetic analysis, fasting plasma insulin and glucose concentrations were adjusted for a number of covariates (sex and age and their interactions, smoking behavior, and menopausal status) using standard regression methods. Residuals from this regression analysis were then directly normalized using an inverse Gaussian transformation. Associations between these normalized traits and the chosen SNPs were then analyzed by Bayesian quantitative trait nucleotide analysis using SOLAR [27]. In this analysis, all parameter estimations were performed by maximum likelihood under the assumption of a multivariate normality. A formal test of association was obtained by calculating a likelihood ratio test statistic comparing a model in which various regression coefficients for SNPs are held equal against a model in which the parameters are allowed to vary. To account for hidden population stratification, the method of Abecasis et al (2000) [28] was used. This method is incorporated into the SOLAR program analysis, which automatically performs a series of association tests for a given set of SNPs.

3. Results

Previous analyses of Ahi-1 tissue-specific expression revealed predominant mRNA levels in the brain and testes of mice [7,29], but Ahi-1 expression in other insulin-sensitive tissues such as adipose tissue and skeletal muscle depots has not been described to our knowledge. We performed a preliminary analysis of Ahi-1 mRNA expression in an extended range of tissues from one lean NGT *P obesus*, a polygenic animal model of obesity and T2D that displays a range of metabolic phenotypes [19,21]. This bank of tissues has been used in previous studies [30,31], and the purpose of this initial screen was to identify which tissues or tissue regions display predominant Ahi-1 gene expression. As expected, Ahi-1 was expressed throughout the brain regions and in gonad tissues (ovary and testes); but Ahi-1 mRNA levels were also evident in all skeletal muscle groups measured (Fig. 1A). Lower Ahi-1 gene expression was observed in lung, heart, and adrenal gland and in various other tissues. To confirm its predominant expression in *P obesus* skeletal muscle, Ahi-1 mRNA was next analyzed in multiple animals and found to have 4- to 8-fold higher

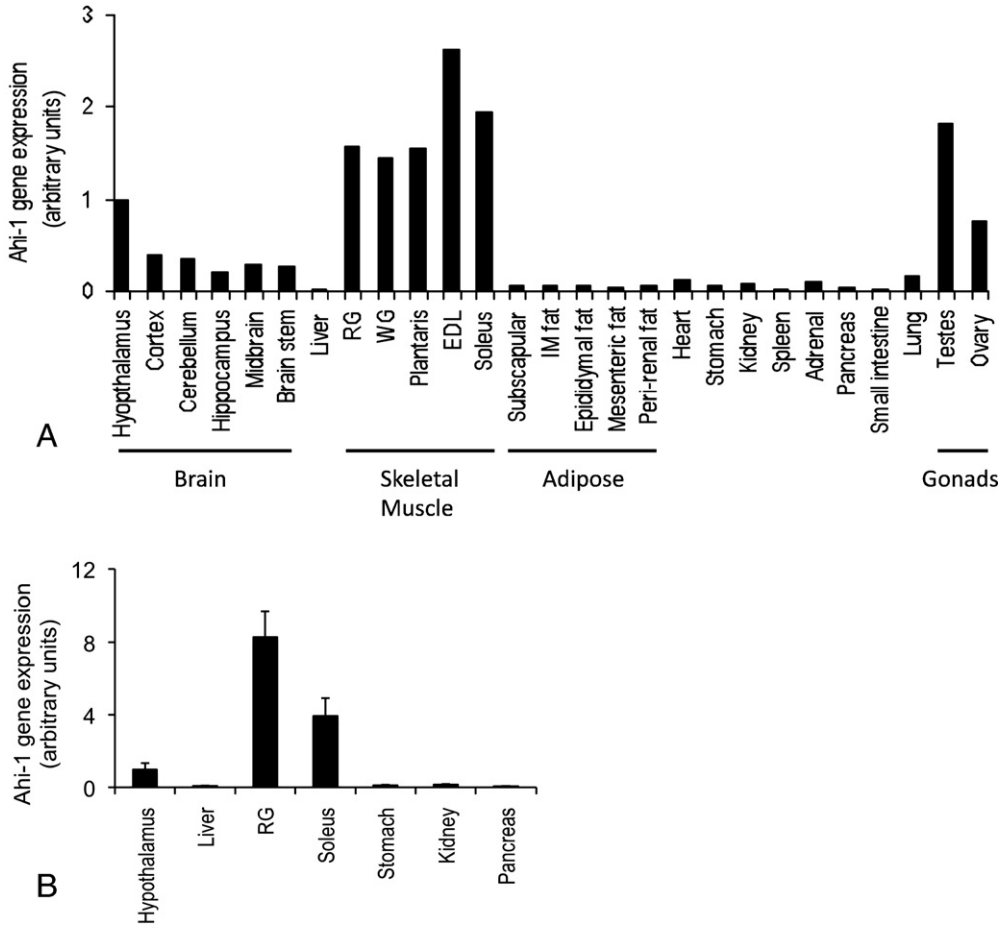

Fig. 1. Distribution of Ahi-1 mRNA in tissues from an 18-week-old male and female (ovary only) lean NGT *P obesus* in the fed state. A, n = 1. B, n = 6 to 7. Values are normalized to hypothalamus gene expression in both figures and expressed as fold-change to the hypothalamus values. RG indicates red gastrocnemius; WG, white gastrocnemius; EDL, extensor digitorum longus; IM, intramuscular.

expression in the soleus and red gastrocnemius skeletal muscles, respectively, compared with the hypothalamus, which, in turn, displayed at least a 6-fold higher level of Ahi-1 gene expression than in liver, mesenteric fat, kidney, stomach, and pancreatic tissues (Fig. 1B).

Ahi-1 gene expression in red gastrocnemius muscle from both fed and 24-hour–fasted NGT, IGT, and T2D *P obesus* animals was next examined (see Table 1 for phenotypic characteristics). Ahi-1 mRNA levels between the fed groups were not found to be significantly different, although the T2D animals tended to display decreased expression compared with the NGT groups ($P = .073$, Fig. 2A). After 24 hours of fasting, Ahi-1 gene expression was reduced

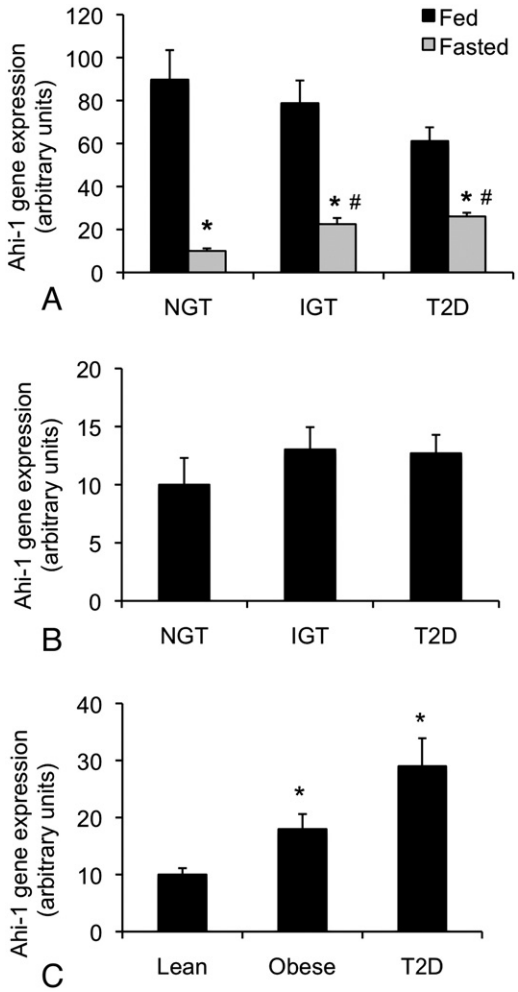

Fig. 2. Analysis of Ahi-1/AHI1 gene expression in *P obesus* and human skeletal muscle tissues. A, Fold-change in Ahi-1 mRNA levels in red gastrocnemius from fed (black bars) and fasted (gray bars) NGT, IGT, and T2D *P obesus* animals (n = 6-7 animals per group). *$P < .001$ from fed NGT and #$P < .002$ from fasted NGT. B, Fold-change in Ahi-1 mRNA levels in mesenteric fat from NGT, IGT, and T2D fasted animals (n = 6-7 animals per group) C, Fold-change in human AHI1 mRNA levels in vastus lateralis muscle from lean, obese, and T2D fasted subjects. (n = 9-13 individuals per group). *$P < .02$ from lean subjects. Values are normalized to cyclophilin gene expression in both figures and expressed as fold-change to NGT or lean values.

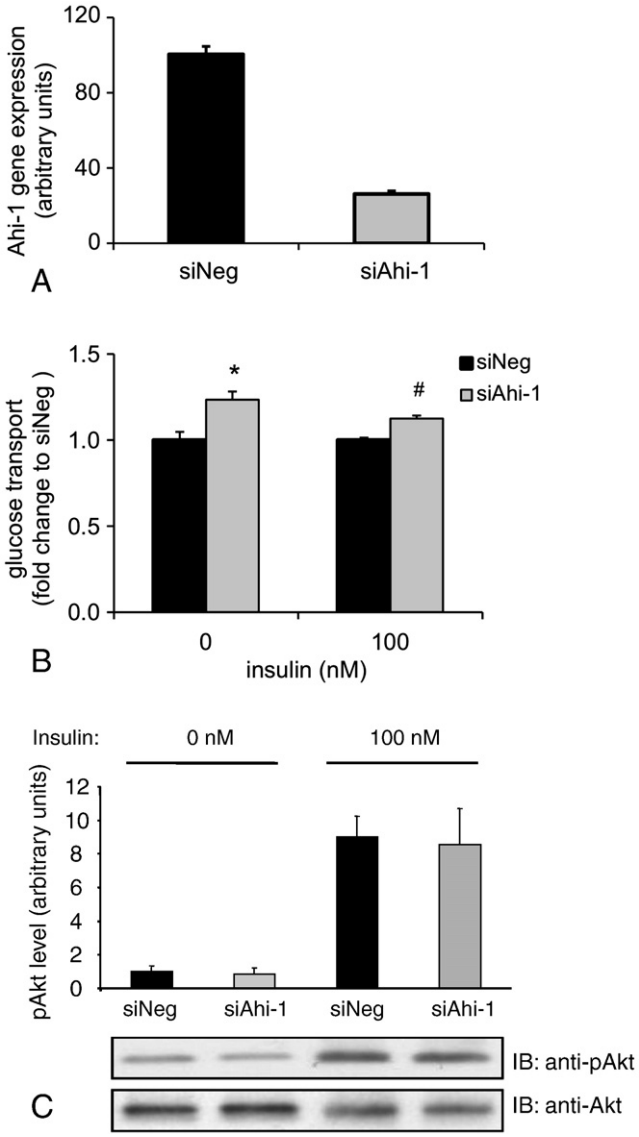

Fig. 3. Glucose transport and phospho-Akt levels in Ahi-1–deficient L6 myotubes. A, Ahi-1 gene expression after transfection with the negative control siRNA (siNeg) and Ahi-1–specific (siAhi-1) siRNAs. Values are normalized to cyclophilin gene expression and expressed as a percentage to siNeg. B, Glucose transport assay in siNeg- (black bars) and siAhi-1– (gray bars) transfected myotubes in both the basal (0 nmol/L insulin) and insulin-stimulated (100 nmol/L insulin) states. Data are expressed as fold-change to siNeg controls (n = 5-6 wells per treatment condition), and 3 independent experiments were performed. *$P < .01$ from basal siNeg and #$P < .001$ from insulin-stimulated siNeg. C, Immunoblotting analysis of Akt and phospho-Akt (ser473) levels in L6 myotubes transfected with siNeg (black bars) or siAhi-1 (gray bars) with or without 15 minutes of insulin treatment. Top panel represents results of the mean ± SEM from 4 independent experiments. Values are normalized to total Akt protein levels and are expressed relative to siNeg at 0 nmol/L. IB indicates immunoblotting.

significantly in all groups ($P < .001$); however, Ahi-1 gene expression in both the IGT and T2D animal groups remained significantly greater compared with the fasted NGT animals with nearly a 3-fold difference observed ($P < .002$, Fig. 2A). This result appeared specific for at least this skeletal muscle group, as no significant difference in Ahi-1 gene expression

Table 3
Association between *AHI1* genetic variants and fasting glucose levels in Mexican Americans subjects

SNP	Nucleotide variation	Exon/Intron	MAF	*P* value
rs17064526	A/C	Intron 10	0.0207	.6284
rs1535436	A/G	Intron 10	0.0251	.2208
rs717120	C/T	Intron 12	0.0699	.7742
rs1535435	A/G	Intron 14	0.0856	.7331
rs737561	C/T	Intron 14	0.0704	.7251
rs11154801	A/C	Intron 19	0.2846	.1528
rs17778438	A/G	Intron 20	0.0482	.9823
rs13208164	A/G	Intron 21	0.0982	.5778
rs2614265	A/G	Intron 22	0.3342	.0360*
rs17064440	A/G	Intron 23	0.0077	.599
rs7772681	C/T	Intron 23	0.3781	.4119
rs2064430	C/T	Intron 24	0.3474	.2699
rs6904731	G/A	Intron 25	0.0217	.0024†
rs6931735	A/G	Intron 25	0.3498	.2021
rs2207000	C/T	Intron 25	0.1298	.2652
rs9285480	C/T	Intron 26	0.0598	.8639
rs7766656	A/G	Intron 26	0.0918	.607
rs1052502	C/T	3′UTR	0.0931	.619

MAF indicates minor allele frequency.
* Nominal association $P < .05$.
† $P <$ target α level .00465 for an experiment-wide significance after adjusting for multiple testing.

was found in mesenteric fat (Fig. 2B) or liver (data not shown) tissues from the same fasted *P obesus* groups. To confirm the finding in the *P obesus*, AHI1 gene expression in vastus lateralis skeletal muscle from lean, obese, and T2D human subjects fasted for 12 to 18 hours was also quantitated. AHI1 was found to be up-regulated significantly by 3-fold in both the obese ($P = .02$) and T2D ($P < .001$) groups compared with lean individuals (Fig. 2C). See Table 2 for the subjects' relevant phenotypic characteristics.

The role of Ahi-1 in myotube insulin sensitivity and/or glucose metabolism was next investigated after the suppression of endogenous Ahi-1 transcripts using Ahi-1–specific siRNA (siAhi-1) in rat L6 myotubes. Ahi-1 gene expression levels were reduced by 75% when compared with the siNeg-transfected myotubes after transfection of siAhi-1 (Fig. 3A). After the measurement of 2-deoxyglucose transport in the transfected myotubes, reduced levels of Ahi-1 resulted in glucose transport increasing by 23% and by 9% in the basal and insulin-stimulated siAhi-1–transfected myotubes, respectively, compared with their siNeg control counterparts ($P < .01$, Fig. 3B). Insulin stimulation typically caused a 1.4- to 1.8-fold increase in glucose transport in relation to unstimulated myotubes (data not shown). Total protein and phosphorylated Akt levels in either the basal or insulin-stimulated state were not affected by reduced Ahi-1 levels (Fig. 3C).

To further investigate the possibility that genetic variation in AHI1 may contribute to the development of T2D, 18 nonredundant AHI1 SNPs were genotyped in a sample of Mexican American subjects. An association between the AHI1 SNP, rs6904731, and fasting blood glucose levels in these subjects was observed ($P = .0024$), which remained

Table 4
Mean normalized fasting plasma glucose values for each genotype

SNP	*P* value	AA	AG	GG
rs2614265	.036	0.325 ± 0.096	0.458 ± 0.089	0.590 ± 0.121
rs6904731	.0024	0.446 ± 0.086	−0.112 ± 0.192	−0.670 ± 0.365

significant after adjusting for multiple testing (target $\alpha P <$ .0047). This uncommon SNP (minor allele frequency = 0.022) is located in intron 25 (Table 3) and accounts for 2.9% of the phenotypic variation in fasting blood glucose levels in these subjects. A nominally significant association with fasting blood glucose levels ($P = .036$) was additionally identified for another SNP, rs2614265, located in intron 22 (Table 3). The direction of effect of rs6904731 and rs2614265 with mean normalized fasting plasma glucose levels for each genotype is outlined in Table 4.

4. Discussion

Here, we provide novel biological evidence for a role for Ahi-1/AHI1 in skeletal muscle. Elevated Ahi-1/AHI1 gene expression was measured in skeletal muscle from both insulin-resistant/obese and T2D *P obesus* and human subjects. Moreover, we show that suppression of Ahi-1 enhanced glucose transport in basal and insulin-stimulated L6 myotubes. We also identified 2 new AHI1 genetic variants associated with fasting blood glucose levels in a sample of Mexican American subjects.

Elevated expression of Ahi-1 mRNA in skeletal muscle compared with other *P obesus* tissues suggests a biological role in this tissue. To our knowledge, the investigation of Ahi-1/AHI1 mRNA or protein expression levels in skeletal muscle from any species has not been reported. Species differences in some spatial and temporal expression of Ahi-1/AHI1 levels from mouse and human brain regions have been noted [29]; but as moderate Ahi-1 gene expression in both brain and gonads tissues was measured in *P obesus*, which has also been described in other species [7,32,33], Ahi-1 gene expression in skeletal muscle is potentially conserved between orthologs. The increased level of skeletal muscle Ahi-1 gene expression in insulin-resistant/obese and T2D animals and humans compared with the lean and healthy groups in the fasted state also reveals that the regulation of Ahi-1/AHI1 transcription is altered in response to fasting in these groups displaying dysregulated metabolic conditions. Furthermore, as fasting causes higher rates of fatty acid oxidation, elevated free fatty acids, and reduced glucose disposal in skeletal muscle (reviewed by Roden [34]), these effects in conjunction with metabolic syndrome conditions appear to increase Ahi-1/AHI1 expression, which, in turn, could indicate that Ahi-1/AHI1 negatively regulates insulin sensitivity and/or glucose metabolism.

The outcome of the glucose transport studies performed after suppression of endogenous Ahi-1 mRNA in L6

myotubes appears to support the premise of Ahi-1 functioning as a negative regulator of glucose uptake. How Ahi-1 may function to do this is not yet clear. We were unable to detect any change in the total level of Akt protein or in its phosphorylated state, and so Ahi-1 may be affecting Akt-independent glucose transport pathways such as through Rac1 [35]. There are multiple glucose transporters (GLUT1, GLUT3, and GLUT4) present in L6 muscle cells [36]; and whether Ahi-1 regulates their expression and/or activities, directly or indirectly, remains to be determined. However, it is of interest to note the recent publication describing a specific mode of action for Ahi-1 in the regulation of ciliogenesis and vesicle trafficking via the GTPase Rab8A [37]. Given that Rab8A appears to be one of the key modulators of GLUT4 vesicle recruitment and fusion in L6 myotubes [38,39], it will be of interest to determine if Ahi-1 is involved in Rab8A/GLUT4 activity and hence glucose transport in skeletal muscle.

The identification of novel AHI1 intronic SNPs, rs6904731 and rs2614265, associated with fasting blood levels in Mexican Americans in this study contributes further to the findings of past GWAS and linkage studies linking AHI1 to a range of metabolic syndrome phenotypes [12-16] and again suggests that AHI1 is a gene associated with increased susceptibility to dysregulated glucose metabolism and T2D. One of the 18 SNPs we tested in this study, rs1535435, was previously found to be associated with T2D [16]; but similarly to a follow-up study investigating the association of this SNP with a range of T2D-related metabolic traits [18], we were not able to find this specific SNP to be significantly associated with fasting blood glucose levels in our population of Mexican Americans. The reasons for lack of replication may be several-fold including variation in patterns of linkage disequilibrium and the genetic basis of their quantitative trait variation, which may be due to ethnicity differences, sample size differences between the cohorts resulting in varying statistical power, and different design strategies. As all these SNPs are intronic, they may also be exerting weak effects on metabolic traits that are not easily replicated.

Our study describes novel biological evidence of a role for AHI1 in skeletal muscle, a key metabolic tissue that is responsible for the majority of peripheral glucose uptake [40]. In addition, it identifies further genetic links associated with metabolic syndrome phenotypes. Together, these data provide a link for AHI1 to the maintenance of glucose homeostasis and T2D progression.

Acknowledgment

We thank Petra Gran, Marissa Trenerry, and Rani Watts for their efforts in preparing and analyzing the clinical samples; and we are grateful to the participants in the San Antonio Family Heart Study. This study was funded by Verva Pharmaceuticals and by the Molecular Medicine and Nutrition Cluster, Deakin University. The SOLAR statistical genetics computer package is supported by a grant from the US National Institute of Mental Health (MH059490).

References

[1] Hanlon L, Barr NI, Blyth K, Stewart M, Haviernik P, Wolff L, et al. Long-range effects of retroviral insertion on c-myb: overexpression may be obscured by silencing during tumor growth in vitro. J Virol 2003;77:1059-68.

[2] Jiang X, Zhao Y, Chan WY, Vercauteren S, Pang E, Kennedy S, et al. Deregulated expression in Ph+ human leukemias of AHI-1, a gene activated by insertional mutagenesis in mouse models of leukemia. Blood 2004;103:3897-904.

[3] Amann-Zalcenstein D, Avidan N, Kanyas K, Ebstein RP, Kohn Y, Hamdan A, et al. AHI1, a pivotal neurodevelopmental gene, and C6orf217 are associated with susceptibility to schizophrenia. Eur J Hum Genet 2006;14:1111-9.

[4] Ingason A, Sigmundsson T, Steinberg S, Sigurdsson E, Haraldsson M, Magnusdottir BB, et al. Support for involvement of the AHI1 locus in schizophrenia. Eur J Hum Genet 2007;15:988-91.

[5] Parisi MA, Doherty D, Chance PF, Glass IA. Joubert syndrome (and related disorders). Eur J Hum Genet 2007;15:511-21.

[6] Valente EM, Brancati F, Silhavy JL, Castori M, Marsh SE, Barrano G, et al. AHI1 gene mutations cause specific forms of Joubert syndrome-related disorders. Ann Neurol 2006;59:527-34.

[7] Jiang X, Hanna Z, Kaouass M, Girard L, Jolicoeur P. Ahi-1, a novel gene encoding a modular protein with WD40-repeat and SH3 domains, is targeted by the Ahi-1 and Mis-2 provirus integrations. J Virol 2002; 76:9046-59.

[8] Kay BK, Williamson MP, Sudol M. The importance of being proline: the interaction of proline-rich motifs in signaling proteins with their cognate domains. Faseb J 2000;14:231-41.

[9] Li D, Roberts R. WD-repeat proteins: structure characteristics, biological function, and their involvement in human diseases. Cell Mol Life Sci 2001;58:2085-97.

[10] Pawson T, Olivier P, Rozakis-Adcock M, McGlade J, Henkemeyer M. Proteins with SH2 and SH3 domains couple receptor tyrosine kinases to intracellular signalling pathways. Philos Trans R Soc Lond B Biol Sci 1993;340:279-85.

[11] Zhou LL, Zhao Y, Ringrose A, DeGeer D, Kennah E, Lin AE, et al. AHI-1 interacts with BCR-ABL and modulates BCR-ABL transforming activity and imatinib response of CML stem/progenitor cells. J Exp Med 2008;205:2657-71.

[12] Xiang K, Wang Y, Zheng T, Jia W, Li J, Chen L, et al. Genome-wide search for type 2 diabetes/impaired glucose homeostasis susceptibility genes in the Chinese: significant linkage to chromosome 6q21-q23 and chromosome 1q21-q24. Diabetes 2004;53:228-34.

[13] Arya R, Blangero J, Williams K, Almasy L, Dyer TD, Leach RJ, et al. Factors of insulin resistance syndrome–related phenotypes are linked to genetic locations on chromosomes 6 and 7 in nondiabetic Mexican-Americans. Diabetes 2002;51:841-7.

[14] Duggirala R, Blangero J, Almasy L, Arya R, Dyer TD, Williams KL, et al. A major locus for fasting insulin concentrations and insulin resistance on chromosome 6q with strong pleiotropic effects on obesity-related phenotypes in nondiabetic Mexican Americans. Am J Hum Genet 2001;68:1149-64.

[15] Stern MP, Duggirala R, Mitchell BD, Reinhart LJ, Shivakumar S, Shipman PA, et al. Evidence for linkage of regions on chromosomes 6 and 11 to plasma glucose concentrations in Mexican Americans. Genome Res 1996;6:724-34.

[16] Salonen JT, Uimari P, Aalto JM, Pirskanen M, Kaikkonen J, Todorova B, et al. Type 2 diabetes whole-genome association study in four populations: the DiaGen consortium. Am J Hum Genet 2007;81: 338-45.

[17] Frayling TM. Genome-wide association studies provide new insights into type 2 diabetes aetiology. Nat Rev Genet 2007;8:657-62.

[18] Holmkvist J, Anthonsen S, Wegner L, Andersen G, Jorgensen T, Borch-Johnsen K, et al. Polymorphisms in AHI1 are not associated with type 2 diabetes or related phenotypes in Danes: non-replication of a genome-wide association result. Diabetologia 2008;51:609-14.

[19] Barnett M, Collier GR, Collier FM, Zimmet P, O'Dea K. A cross-sectional and short-term longitudinal characterisation of NIDDM in *Psammomys obesus*. Diabetologia 1994;37:671-6.

[20] Walder K, Oakes N, Fahey RP, Cooney G, Zimmet PZ, Collier GR. Profile of dyslipidemia in *Psammomys obesus*, an animal model of the metabolic syndrome. Endocr Regul 2002;36:1-8.

[21] Walder KR, Fahey RP, Morton GJ, Zimmet PZ, Collier GR. Characterization of obesity phenotypes in *Psammomys obesus* (Israeli sand rats). Int J Exp Diabetes Res 2000;1:177-84.

[22] Olefsky JM. Mechanisms of the ability of insulin to activate the glucose-transport system in rat adipocytes. Biochem J 1978;172: 137-45.

[23] Foletta VC, Prior MJ, Stupka N, Carey K, Segal DH, Jones S, et al. NDRG2, a novel regulator of myoblast proliferation, is regulated by anabolic and catabolic factors. J Physiol 2009;587:1619-34.

[24] Mitchell BD, Kammerer CM, Blangero J, Mahaney MC, Rainwater DL, Dyke B, et al. Genetic and environmental contributions to cardiovascular risk factors in Mexican Americans. The San Antonio Family Heart Study. Circulation 1996;94:2159-70.

[25] Boerwinkle E, Chakraborty R, Sing CF. The use of measured genotype information in the analysis of quantitative phenotypes in man. I. Models and analytical methods. Ann Hum Genet 1986;50:181-94.

[26] Li J, Ji L. Adjusting multiple testing in multilocus analyses using the eigenvalues of a correlation matrix. Heredity 2005 Sep;95:221-7.

[27] Blangero J, Goring HH, Kent Jr JW, Williams JT, Peterson CP, Almasy L, et al. Quantitative trait nucleotide analysis using Bayesian model selection. Hum Biol 2005;77:541-59.

[28] Abecasis GR, Cookson WO, Cardon LR. Pedigree tests of transmission disequilibrium. Eur J Hum Genet 2000;8:545-51.

[29] Doering JE, Kane K, Hsiao YC, Yao C, Shi B, Slowik AD, et al. Species differences in the expression of Ahi1, a protein implicated in the neurodevelopmental disorder Joubert syndrome, with preferential accumulation to stigmoid bodies. J Comp Neurol 2008;511:238-56.

[30] Bozaoglu K, Bolton K, McMillan J, Zimmet P, Jowett J, Collier G, et al. Chemerin is a novel adipokine associated with obesity and metabolic syndrome. Endocrinology 2007;148:4687-94.

[31] Trevaskis J, Walder K, Foletta V, Kerr-Bayles L, McMillan J, Cooper A, et al. Src homology 3-domain growth factor receptor-bound 2-like (endophilin) interacting protein 1, a novel neuronal protein that regulates energy balance. Endocrinology 2005;146:3757-64.

[32] Ferland RJ, Eyaid W, Collura RV, Tully LD, Hill RS, Al-Nouri D, et al. Abnormal cerebellar development and axonal decussation due to mutations in AHI1 in Joubert syndrome. Nat Genet 2004;36:1008-13.

[33] Zhou W, Song P. Molecular cloning of a novel gene ZAhi-1 and its expression analysis during zebrafish gametogenesis. Mol Biol Rep 2006;33:111-6.

[34] Roden M. How free fatty acids inhibit glucose utilization in human skeletal muscle. News Physiol Sci 2004;19:92-6.

[35] JeBailey L, Wanono O, Niu W, Roessler J, Rudich A, Klip A. Ceramide- and oxidant-induced insulin resistance involve loss of insulin-dependent Rac-activation and actin remodeling in muscle cells. Diabetes 2007;56:394-403.

[36] Tsakiridis T, McDowell HE, Walker T, Downes CP, Hundal HS, Vranic M, et al. Multiple roles of phosphatidylinositol 3-kinase in regulation of glucose transport, amino acid transport, and glucose transporters in L6 skeletal muscle cells. Endocrinology 1995;136: 4315-22.

[37] Hsiao YC, Tong ZJ, Westfall JE, Ault JG, Page-McCaw PS, Ferland RJ. Ahi1, whose human ortholog is mutated in Joubert syndrome, is required for Rab8a localization, ciliogenesis and vesicle trafficking. Hum Mol Genet 2009;18:3926-41.

[38] Ishikura S, Klip A. Muscle cells engage Rab8A and myosin Vb in insulin-dependent GLUT4 translocation. Am J Physiol Cell Physiol 2008;295:C1016-1025.

[39] Randhawa VK, Ishikura S, Talior-Volodarsky I, Cheng AW, Patel N, Hartwig JH, et al. GLUT4 vesicle recruitment and fusion are differentially regulated by Rac, AS160, and Rab8A in muscle cells. J Biol Chem 2008;283:27208-19.

[40] DeFronzo RA, Gunnarsson R, Bjorkman O, Olsson M, Wahren J. Effects of insulin on peripheral and splanchnic glucose metabolism in noninsulin-dependent (type II) diabetes mellitus. J Clin Invest 1985;76: 149-55.